Acta Biochim Biophys Sin 2026, 58(11): 2515–2528
https://cstr.cn/32197.14.abbs.2026027
https://doi.org/10.3724/abbs.2026027
Original Article

Original Article

PCIF1 modulates glioblastoma cell migration and invasion by altering PI(3,4)P2 levels through the PI5-phosphatase INPP5B

Preethi Priyanka Musunuru[1,2,†], Yihan Li[1,2,†], Yu Zhou[1,2,†], Gai Liu[1,2], Zhuang Sha[1], Zhiyuan Hu[2], Junbo Zhou[2], Naveena Konduru[3], Qingming Meng[1,*], Shangfeng Gao[1,2,*], and Rutong Yu[1,2,*]

[1]Department of Neurosurgery, The Affiliated Hospital of Xuzhou Medical University, Xuzhou 221002, China, [2]Institute of Nervous System Diseases, Xuzhou Medical University, Xuzhou 221002, China, and [3]Department of Otorhinolaryngology-Head and Neck Surgery, The Affiliated Hospital of Xuzhou Medical University, Xuzhou 221002, China

[†]These authors contributed equally to this work.

*Correspondence address. E-mail: yunfan661@163.com (Q.M.); gaoshangfeng@xzhmu.edu.cn (S.G.); yu.rutong@163.com (R.Y.)

Received 12 August 2025 Accepted 10 December 2025 Published 9 May 2026

Abstract

Phosphorylated CTD Interacting Factor 1 (PCIF1) is the exclusive methyltransferase responsible for the N6,2-O-dimethyladenosine (m^6Am) modification in mammalian mRNA. Our previous research identified PCIF1 as a potent tumor suppressor in glioma, demonstrating its ability to impair cell proliferation, induce G2/M phase arrest, and promote apoptosis. However, its role in glioma cell migration and invasion remains unclear. In this study, we investigate how PCIF1 regulates glioma cell migration and invasion. Overexpression of PCIF1 inhibits migration and invasion, whereas *PCIF1* knockdown enhances these behaviors. Corresponding changes are observed in mesenchymal markers (Vimentin, β-catenin, Snail, Slug) and the epithelial marker T-cadherin, indicating that PCIF1 suppresses epithelial-to-mesenchymal transition (EMT)-mediated glioma invasion. Mechanistically, PCIF1 modulates the AKT pathway by promoting proteasomal degradation of AKT while increasing phosphorylated AKT (p-AKT) levels, revealing a complex regulatory mechanism. *PCIF1* knockdown upregulates INPP5B, a lipid phosphatase, causing accumulation of PI(3,4)P2 and enhanced AKT activation. Conversely, PCIF1 overexpression increases PI(3,4,5)P3 production, elevating p-AKT levels. This bidirectional regulation suggests that PCIF1 influences phosphoinositide signaling and AKT activation. Our findings highlight PCIF1 as a key modulator of glioblastoma cell migration and invasion through phosphoinositide signaling, positioning it as a potential biomarker and therapeutic target in glioma.

Key words PCIF1, glioblastoma, invasion, INPP5B

Introduction

Gliomas represent the most common type of primary intracranial tumors, accounting for approximately 48% of all primary malignant central nervous system (CNS) tumors. Among gliomas, glioblastoma multiforme (GBM) is the most aggressive and lethal subtype, characterized by rapid proliferation, diffuse infiltration into surrounding tissues, and a high recurrence rate after surgical resection [1]. The highly invasive nature of GBM significantly hampers effective treatment and is a major contributor to its dismal clinical outcomes [2,3]. One of the key drivers of GBM progression is the dysregulation of critical signaling pathways, particularly AKT signaling, which is frequently activated in these tumors [4,5]. The aberrant activation of AKT signaling plays a central role in promoting tumor growth, survival, and resistance to therapies [6,7]. Although several drugs targeting AKT signaling have been developed, their clinical success has been limited due to challenges such as drug resistance, activation of compensatory signaling pathways, and the complexity of the tumor microenvironment [8]. The gap in knowledge remains in understanding the precise molecular mechanisms by which this pathway is regulated, and

© The Author(s) 2026. This is an open access article distributed under the terms of the Creative Commons Attribution-NonCommercial-NoDerivs License (https://creativecommons.org/licenses/by-nc-nd/4.0/).

this study aims to bridge that gap, offering insights into potential novel therapeutic targets for GBM treatment.

PCIF1, also known as cap-specific adenosine methyltransferase (CAPAM), is a critical enzyme responsible for m^6Am modification in mammalian mRNA [9–11]. Structurally, PCIF1 contains a conserved N-terminal WW domain, two nuclear localization sequences (NLS) at the amino- and carboxyl-termini, and a conserved NPPF motif near the carboxyl-terminus that is essential for its m^6Am methyltransferase activity [9–11]. The WW domain can bind to the phosphorylated C-terminal domain (CTD) of RNA polymerase II, potentially influencing transcriptional regulation, signaling, and cytoskeletal dynamics. These structural features suggest that PCIF1 may exert complex regulatory effects beyond its methyltransferase activity [11]. The m^6Am modification plays a key role in regulating mRNA stability and translation efficiency, which in turn influences gene expression profiles associated with tumor progression in various cancers, including head and neck squamous cell carcinoma and gastric, renal and colorectal cancers, where PCIF1 promotes tumor growth and invasion [12–15]. In contrast, it acts as a tumor suppressor in bladder cancer, neuroblastoma, and melanoma [16–18]. Specifically, in bladder cancer, loss of PCIF1 enhances colony formation and tumor growth [16]; in neuroblastoma, m^6Am modification promotes differentiation and reduces oncogenic potential [17]; and in melanoma, PCIF1 loss alters mRNA methylation patterns, contributing to tumor progression [18]. These findings highlight the context-dependent roles of PCIF1 and the complexity of its function, underscoring the novelty of investigating its functional mechanisms in glioma. Our previous study demonstrated an inverse correlation between PCIF1 expression and glioma grade, along with an inhibitory effect of PCIF1 on cell survival and proliferation, both *in vitro* and *in vivo* [19]. However, the molecular mechanisms by which PCIF1 regulates glioma migration, invasion, EMT, and AKT signaling remain largely unexplored.

The AKT signaling pathway is frequently dysregulated in glioblastoma, leading to enhanced cell survival, proliferation, and migration [6,7]. A critical modulator of this pathway is INPP5B, which dephosphorylates the phosphoinositide PI(3,4,5)P3, thereby regulating the level of PI(3,4)P2, a key lipid involved in cellular motility, cytoskeletal dynamics, and invasion [20]. Reduced level of PI(3,4)P2 has been shown to suppress glioma cell migration and invasion, particularly in cells with disrupted tumor suppressor mechanisms [21]. This highlights the importance of precise regulation of AKT signaling in glioma progression, particularly with regard to invasion and metastasis.

In this study, we aimed to further elucidate the role of PCIF1 in GBM pathophysiology, with a specific focus on its involvement in regulating cell migration, invasion, and EMT. We hypothesize that PCIF1 modulates key cellular processes essential for GBM invasion and metastasis through its effects on AKT signaling and the phosphatase INPP5B. Our previous and current findings suggest that PCIF1 plays a critical role in glioma cell progression, and this study seeks to provide deeper insights into its molecular mechanisms. By understanding how PCIF1 regulates AKT signaling and its downstream effectors, we hope to uncover novel therapeutic strategies targeting PCIF1 for the treatment of GBM.

Materials and Methods

Cell lines and cell culture

The HEK293T cell line, along with the glioma cell lines T98G, U251, and U87, were obtained from the Shanghai Cell Bank, Type Culture Collection Committee, Chinese Academy of Sciences (Shanghai, China). GBM-Y2 is a primary glioma cell line derived from surgical specimens of an IDH1-wild-type GBM patient as detailed in our previous studies [19,22]. All cell lines were cultured in Dulbecco's modified Eagle's medium (DMEM; HyClone, Logan, USA) supplemented with 10% fetal bovine serum (FBS; Gibco, Grand Island, USA). Cells were maintained at 37°C in a humidified incubator with 5% CO_2.

Lentivirus and plasmids

Short-hairpin RNAs (shRNAs) targeting human *PCIF1* (NM_022104) were cloned into the GV248 vector to generate knockdown plasmids (Genechem, Shanghai, China). The sense target sequences were as follows: scramble: 5′-UUCUCCGAACGUGUCACGU-3′, sh*PCIF1*-1: 5′-CCCUACUACUUCAACCGAU-3′ and sh*PCIF1*-2: 5′-CCUUCCAU GUUUCGUGAAA-3′. The human *PCIF1* coding sequence and the APPA mutant sequence was cloned and inserted into the pLVX-TetOne-Puro vector to construct PCIF1 wild-type and PCIF1 APPA plasmids (Youbio Biological Technology, Changsha, China), respectively. The shRNA-mediated *PCIF1*-downregulated cells and doxycycline (Dox)-inducible PCIF1-overexpressing cells were established using these constructs as described in our prior publication [19]. To induce the expression of wild-type or APPA mutant PCIF1, the cells were treated with Dox (100 ng/mL, Y266887; Beyotime Biotechnology, Shanghai, China) for 24 h.

For transient overexpression of PCIF1, we cloned wild-type PCIF1 (PCIF1-WT), a methyltransferase-deficient mutant (PCIF1-APPA), and a WW domain mutant (PCIF1-S54H) into the pCMV expression vector. The PCIF1-APPA mutant carries point mutations at residues N553A and F556A (NPPF→APPA), while the PCIF1-S54H mutant contains a serine-to-histidine substitution at residue 54 (S54H) within the WW domain. Each construct was fused with a Flag tag for subsequent detection. Similarly, the INPP5B overexpression plasmid (OE-INPP5B) was cloned and inserted into the pCMV vector with a Flag tag for analyses. All plasmids, including those for PCIF1-WT, PCIF1-APPA, PCIF1-S54H, and OE-INPP5B, were provided by Transduction Biology Laboratory (Wuhan, China).

siRNA and plasmid transfection

Custom-designed small interfering RNAs (siRNAs) targeting *INPP5B* were synthesized by General Biosystems (Chuzhou, China). The sequences were as follows: si-*INPP5B3*: 5′-UAG CAUAUUUGGCAGCUUA-3′ and si-*INPP5B4*: 5′-GAUGAAGAGU CUUACUGUA-3′. A non-targeting control siRNA (si-NC) (5′-UUCUCCGAACGUGUCACGU-3′) was also synthesized by the same provider. Glioma cells at 70%–90% confluence in 6-well plates were transfected with siRNAs using Lipofectamine 2000 (Invitrogen, Carlsbad, USA) according to the manufacturer's protocol. Although two siRNAs were designed, only si-*INPP5B4* was used in the subsequent experiments due to its higher knockdown efficiency, which was confirmed by western blot analysis (Supplementary Figure S1).

For plasmid transfection, cells were seeded in 6-cm dishes and transfected at 40%–50% confluence with 2 μg of plasmids using PolyJet (SignaGen, Gaithersburg, USA) following the manufacturer's protocol. Six hours following transfection, the medium was replaced by fresh medium containing 10% FBS, and the cells were incubated for an additional 48 h before further experimentation.

RNA extraction and quantitative real-time PCR

Total RNA was extracted from cells using a commercial kit (Yeasen Biotechnology, Shanghai, China) following the manufacturer's instructions. Two micrograms of total RNA were reverse-transcribed into cDNA using a cDNA synthesis kit (Yeasen Biotechnology) [23]. Quantitative real-time PCR (qRT-PCR) was performed using SYBR Green Master Mix (Yeasen Biotechnology) on an Applied Biosystems 7500 instrument (Applied Biosystems, Foster City, USA), as described in our recent study [19]. The mRNA levels of *PCIF1*, *AKT1*, and *INPP5B* were analyzed using the comparative Ct (ΔΔCt) method and normalized to *β-actin*. The sequences of primers used for qRT-PCR are listed in Supplementary Table S1.

Protein extraction and western blot analysis

GBM cells were lysed in ice-cold RIPA lysis buffer (Beyotime Biotechnology, Shanghai, China) to extract total proteins. Protein concentrations were determined using a BCA protein assay kit (Beyotime Biotechnology) following the manufacturer's instructions. Equal amounts of protein were separated by 10% SDS-PAGE and transferred onto polyvinylidene difluoride (PVDF) membranes (Millipore, Billerica, USA). The membranes were blocked with 3% bovine serum albumin (BSA; 0332; Amresco, Solon, USA) to minimize non-specific binding, followed by overnight incubation at 4°C with primary antibodies. After washing, the membranes were incubated with horseradish peroxidase (HRP)-conjugated secondary antibodies (1:4000; Abcam, Cambridge, UK) for 2 h at room temperature. Protein bands were visualized using Pierce ECL Substrate (Thermo Fisher Scientific, Waltham, USA), and images were captured using the ChemiDoc Touch Imaging System (Bio-Rad, Hercules, USA). Band intensities were quantified using ImageJ software (National Institutes of Health, Bethesda, USA), with relative expression levels normalized to GAPDH. The following primary antibodies were used: PCIF1 (ab205106, 1:2000; Abcam, Cambridge, UK), AKT (2920, 1:2000; Cell Signaling Technology, Danvers, USA), phosphorylated AKT (p-AKT(Ser473), 4060, 1:2000; Cell Signaling Technology), INPP5B (15141-1-AP, 1:1000; Proteintech, Rosemont, USA), β-catenin (8480s, 1:2000; Cell Signaling Technology), T-cadherin (ABT121, 1:1000; Merck Millipore, Billerica, USA), Snail2 (12129-1-AP, 1:1000; Proteintech), Slug (ab180714, 1:1000; Abcam), Vimentin (sc-373717, 1:1000; Santa Cruz Biotechnology, Santa Cruz, USA), GAPDH (60004-1-Ig, 1:20000; Proteintech), HA (51064-2-AP, 1:5000; Proteintech), and β-actin (sc-47778, 1:1500; Santa Cruz Biotechnology).

Scratch assay

To assess cell migration, an *in vitro* wound healing assay was performed. Cells were cultured in 6-well plates until they reached 80%–90% confluence. A consistent scratch was made across the cell monolayer using a sterile 200-μL pipette tip, as previously described [24,25]. Then, the wells were rinsed twice with phosphate-buffered saline (PBS) to remove detached cells. The remaining cells were then maintained in serum-free medium to minimize cell proliferation. Wound closure was evaluated at 0 and 24 h by capturing images at several predetermined positions along the scratch using an IX-71 inverted microscope (Olympus, Tokyo, Japan). The wound area at each time point was quantified using ImageJ software, and the percentage of wound closure was calculated by comparing the wound area at 24 h to the initial wound area at 0 h.

Transwell migration and invasion assays

The migratory and invasive abilities of cells were evaluated using Transwell assays. For the migration assay, 5×10^3 cells suspended in 200 μL of serum-free medium were seeded into the upper chambers of 24-well Transwell inserts with an 8-μm-pore membrane (Corning, Corning, USA). The lower chambers were filled with 600 μL of medium supplemented with 10% FBS to act as a chemoattractant. Cells were allowed to migrate through the membrane for 24 h at 37°C in a humidified atmosphere with 5% CO_2. After incubation, non-migrated cells on the upper side of the membrane were removed with a cotton swab. The migrated cells on the lower surface of the membrane were fixed with 4% paraformaldehyde, stained with crystal violet, and quantified by counting in five random fields under a light microscope [24,25].

For the invasion assay, the upper chamber was coated with Matrigel (356234; BD, Franklin Lakes, USA) to mimic the extracellular matrix. Cells were seeded as described for the migration assay, and invasion was allowed to proceed for 24 to 48 h. After incubation, non-invasive cells were removed, and the invasive cells that had penetrated through the Matrigel and migrated to the lower surface of the membrane were fixed, stained, and counted as described above for the migration assay.

Ubiquitination assay

U87 cells were transiently co-transfected with PCIF1-WT and HA-tagged ubiquitin (HA-Ub) plasmids (Youbio Biological Technology). After 20 h, the cells were treated with 40 μM MG132 for 4 h to inhibit proteasomal degradation. Cells were then lysed on ice for 1 h in protein lysis buffer and centrifuged at 13,000 *g* for 15 min at 4°C to collect the supernatant. Protein A/G magnetic beads (C0104B; TargetMol, Boston, USA) were pre-incubated with AKT antibody (2 μg; Cell Signaling Technology) for 2 h at 4°C, followed by incubation with the cell lysates overnight at 4°C. After extensive washing, the immune complexes were eluted and subjected to western blot (WB) analysis with HA antibody to detect ubiquitinated AKT, as described previously [26].

Immunofluorescence staining

The localization and expression of phosphatidylinositol 3,4,5-trisphosphate [PI(3,4,5)P3] were assessed by immunofluorescence (IF) staining as previously reported [27]. Cells were incubated overnight at 4°C with a mouse anti-PI(3,4,5)P3 primary antibody (Z-P345, 1:100; Echelon Biosciences, Salt Lake City, USA). After thorough washing with PBS, the cells were incubated for 2 h at room temperature in the dark with an Alexa Fluor 594-conjugated anti-mouse secondary antibody (1:200; Invitrogen). For F-actin organization and distribution, cells were stained with TRITC phalloidin (1:200; Invitrogen) for 1 h at room temperature in the dark. The nuclei were counterstained with 4′,6-diamidino-2-phenylindole (DAPI, 1:1000; Sigma-Aldrich, St Louis, USA). Coverslips were mounted using Paramount (Haoran Biological Technology, Shanghai, China), and images were captured under a DM 2500 microscope (Leica, Wetzlar, Germany) for F-actin imaging and under an LSM880 AiryScan confocal microscope (Zeiss, Oberkochen, Germany) for IF imaging. Fluorescence intensity was quantified using ImageJ and used for the analysis of the PI(3,4,5)P3 levels.

PtdIns(3,4)P2 ELISA

Glioma cells (5×10^6) were lysed in 0.5 M trichloroacetic acid to

extract PtdIns(3,4)P2, which was subsequently quantified using a PtdIns(3,4)P2 mass ELISA kit (K-3800; Echelon Biosciences). Briefly, lipids were extracted by incubating the cell lysates with a mixture of methanol, chloroform, and 12 M HCl (80:40:1) for 15 min at room temperature. The lipid mixture was then partitioned by centrifugation after addition of chloroform (0.75 mL) and 0.1 M HCl (1.35 mL). The resulting lower phase was collected, vacuum-dried, and reconstituted in the assay buffer. The extracted lipids, along with standards and controls, were sequentially incubated with the PtdIns(3,4)P2 detector, a secondary detection reagent, and the TMB substrate. The reaction was terminated using 0.5 M H_2SO_4, and the absorbance was measured at 450 nm using a microplate reader (SN 266267; BioTek, Winooski, USA).

Immunohistochemistry (IHC)

Tumor tissues were obtained from previously established intracranial xenograft models as described in our prior publication [19]. Briefly, male athymic BALB/c nude mice (5–6 weeks old, ~20 g) were intracranially implanted with U87 cells expressing shPCIF1-2 (knockdown) or GBM-Y2 cells stably overexpressing PCIF1-WT or APPA. Mice were sacrificed at the same time after tumor implantation, and whole brains were collected for IHC analysis. The animal ethics approval number is 202009A269, approved in September 2020 by the Experimental Animal Ethics Committee of Xuzhou Medical University.

IHC was performed using a similar protocol as described previously [27]. Briefly, antigen retrieval was carried out on tissue sections by heating in citrate buffer (pH 6.0) using a microwave. The sections were then incubated with primary antibodies at the following dilutions: Snail (1:400), Vimentin (1:50), T-cadherin (1:100), and INPP5B (1:200). These primary antibodies are the same as those used for western blot analysis, as described above. After primary antibody incubation, all sections were processed using an ABC kit (Vector Laboratories, Burlingame, USA) following the manufacturer's protocol. Visualization was performed using a DAB substrate solution containing 0.01% hydrogen peroxide, followed by counterstaining with hematoxylin (KeyGEN BioTECH, Nanjing, China). Images were captured using a DM2500 microscope (Leica), and cell counting was performed by capturing three randomly selected high-magnification (40×) images per sample. The total number of cells and positively stained cells were counted by a blinded investigator, and the percentage of positive cells was calculated for statistical analysis [19,27].

Statistical analysis

In vitro experiments were conducted with a minimum of three biological replicates, and data are expressed as the mean ± SEM. Statistical significance between two groups was determined using Student's *t*-test. For multiple group comparisons, one-way analysis of variance (ANOVA) was performed, followed by either Dunnett's or Tukey post hoc tests. All statistical analyses were performed using SPSS version 19.0 (SPSS Inc., Chicago, USA), with a significance threshold set at $P < 0.05$.

Results

Knockdown of *PCIF1* promotes glioma cell migration, invasion, and EMT

To explore the functional role of PCIF1 in glioma cell progression, we first validated its knockdown at both the mRNA and protein levels in U251 and T98G glioma cells. The qPCR confirmed a significant reduction in *PCIF1* mRNA levels following knockdown (Figure 1A), while WB analysis verified a corresponding decrease in PCIF1 protein expression (Figure 1B). Functionally, PCIF1 depletion significantly enhanced glioma cell motility and invasiveness. The scratch assay demonstrated that *PCIF1* knockdown accelerated wound closure at the 24 h time point, indicating increased migratory capacity (Figure 1C,D). Consistently, Transwell migration assays revealed a substantial rise in the number of migrating cells upon *PCIF1* knockdown. Similarly, Transwell invasion assays showed a marked increase in the invasive potential of PCIF1-deficient glioma cells (Figure 1E–G). To further investigate the cellular mechanisms driving the enhanced migratory and invasive potential of PCIF1-depleted glioma cells, we employed TRITC phalloidin staining to assess actin cytoskeletal reorganization in U251 cells. *PCIF1* knockdown induced distinct cytoskeletal changes, including increased actin stress fibers and the formation of prominent membrane protrusions, such as filopodia and lamellipodia [28] (Supplementary Figure S2). Given the well-established role of EMT in glioma progression, we next examined key EMT markers. WB analysis revealed that *PCIF1* knockdown reduced the epithelial marker T-cadherin, which we used as a surrogate epithelial marker because E-cadherin is expressed at very low levels in glioma cells [29], while mesenchymal markers, including Vimentin, β-catenin, Snail, and Slug, were upregulated (Figure 1H). To further validate these findings *in vivo*, we performed IHC staining using EMT-related antibodies on xenograft tumor sections obtained from our previous study [19]. Consistent with the *in vitro* results, IHC staining demonstrated reduced T-cadherin expression and increased levels of Vimentin and Snail in PCIF1-deficient tumors (Figure 1I,J). Collectively, these findings indicate that *PCIF1* knockdown promotes glioma cell migration and invasion, which is accompanied by changes in the cytoskeleton and EMT.

PCIF1 overexpression suppresses glioma cell migration, invasion, and EMT

To investigate the role of PCIF1 in glioma progression, we established PCIF1-overexpressing GBM-Y2 and U87 glioma cell lines. Cells were treated with 100 ng/mL Dox to induce the expression of PCIF1-WT and -APPA. The qPCR analysis confirmed a significant increase in *PCIF1* mRNA expression in PCIF1-overexpressing cells (Figure 2A), while WB analysis verified a corresponding elevation in PCIF1 protein levels (Figure 2B). Next, we assessed the impact of PCIF1 overexpression on glioma cell migration and invasion. Scratch assays in GBM-Y2 cells were conducted, and wound closure was observed under PCIF1 overexpression and control conditions, with PCIF1-overexpressing cells exhibiting a reduced migratory capacity at the 24 h time point (Figure 2C,D). Similarly, Transwell migration and invasion assays in PCIF1-overexpressing GBM-Y2 and U87 cells revealed a significant reduction in migrating and invading cells compared to controls (Figure 2E–G). These findings suggest that PCIF1 overexpression suppresses glioma aggressiveness. To explore the underlying mechanisms, we examined EMT marker expression following PCIF1 overexpression. WB analysis demonstrated a marked increase in the epithelial marker T-cadherin and a significant downregulation of mesenchymal markers, including Vimentin, β-catenin, Snail, and Slug (Figure 2H). To validate these

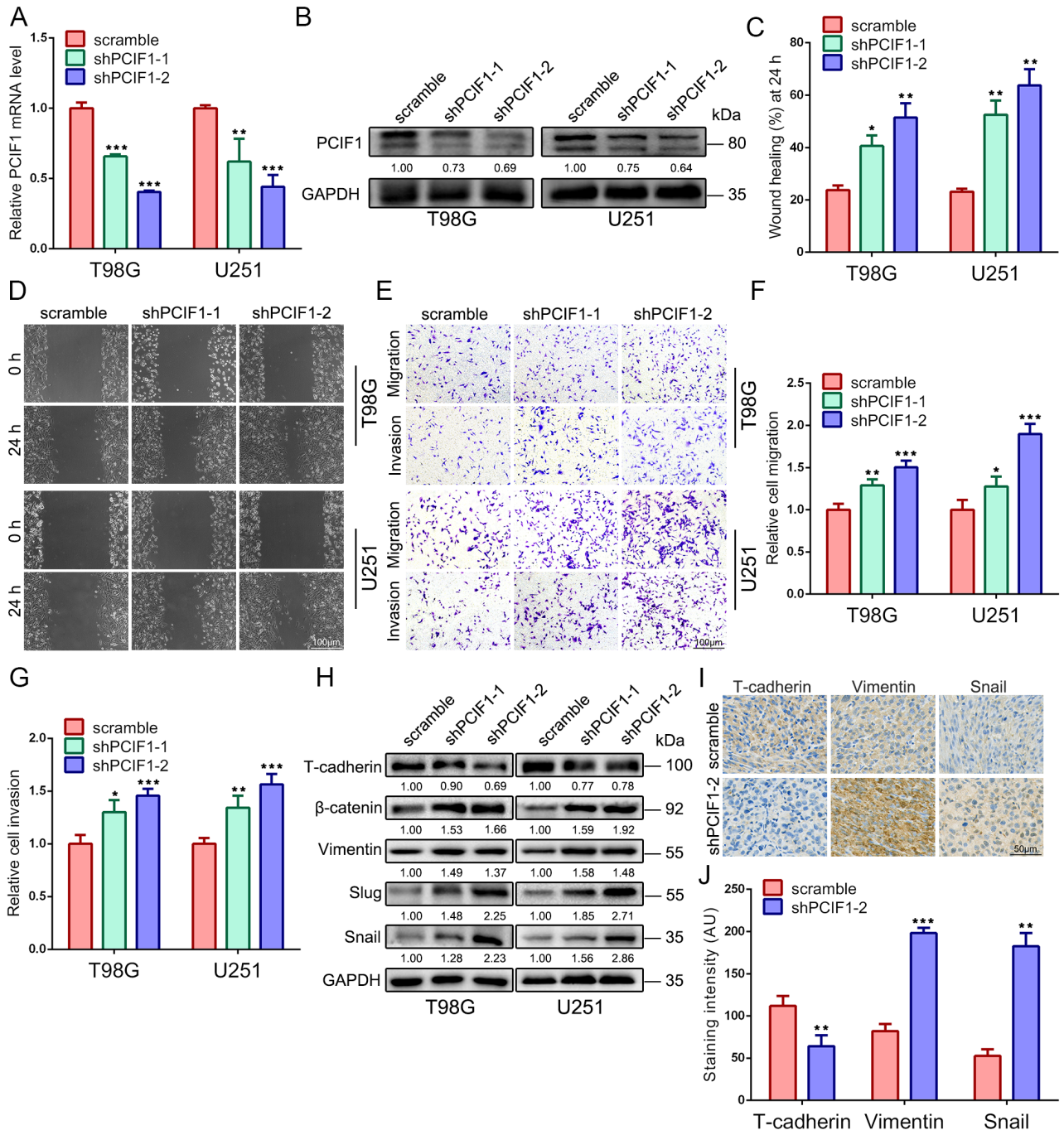


Figure 1. Effect of *PCIF1* knockdown on glioma cell migration, invasion, and EMT activation (A) qRT-PCR analysis of *PCIF1* mRNA expression in T98G and U251 cells following *PCIF1* knockdown. (B) WB analysis showing PCIF1 protein levels in T98G and U251 cells following *PCIF1* knockdown. (C,D) Scratch assay images of T98G and U251 cells with *PCIF1* knockdown at the 24 h time point, with quantification of wound healing percentage (C) and representative images (D). Scale bar = 100 μm. (E–G) Transwell migration and invasion assays assessing the migratory and invasive capacity of T98G and U251 cells following *PCIF1* knockdown, with representative images (E) and quantification of relative cell numbers (F,G). Scale bar = 100 μm. (H) WB analysis of EMT markers in T98G and U251 cells following *PCIF1* knockdown. (I,J) IHC staining of EMT markers in tumor samples from PCIF1-depleted glioma tissues, with representative images (I) and quantification of staining intensity (J). Scale bar = 50 μm for IHC images. Data are presented as the mean ± SEM of three independent experiments. Statistical significance compared to control groups is indicated by $*P < 0.05$, $**P < 0.01$, and $***P < 0.001$.

findings *in vivo*, we performed IHC staining on tumor samples from our previously published study [19]. Consistent with our *in vitro* results, IHC analysis revealed increased T-cadherin expression and decreased Vimentin levels in PCIF1-overexpressing tumors (Figure 2I,J). Interestingly, no significant differences were observed between PCIF1-WT and the -APPA mutant in their effects on migration and invasion. This suggests that the inhibitory effect of PCIF1 on glioma cell motility and invasiveness is not entirely

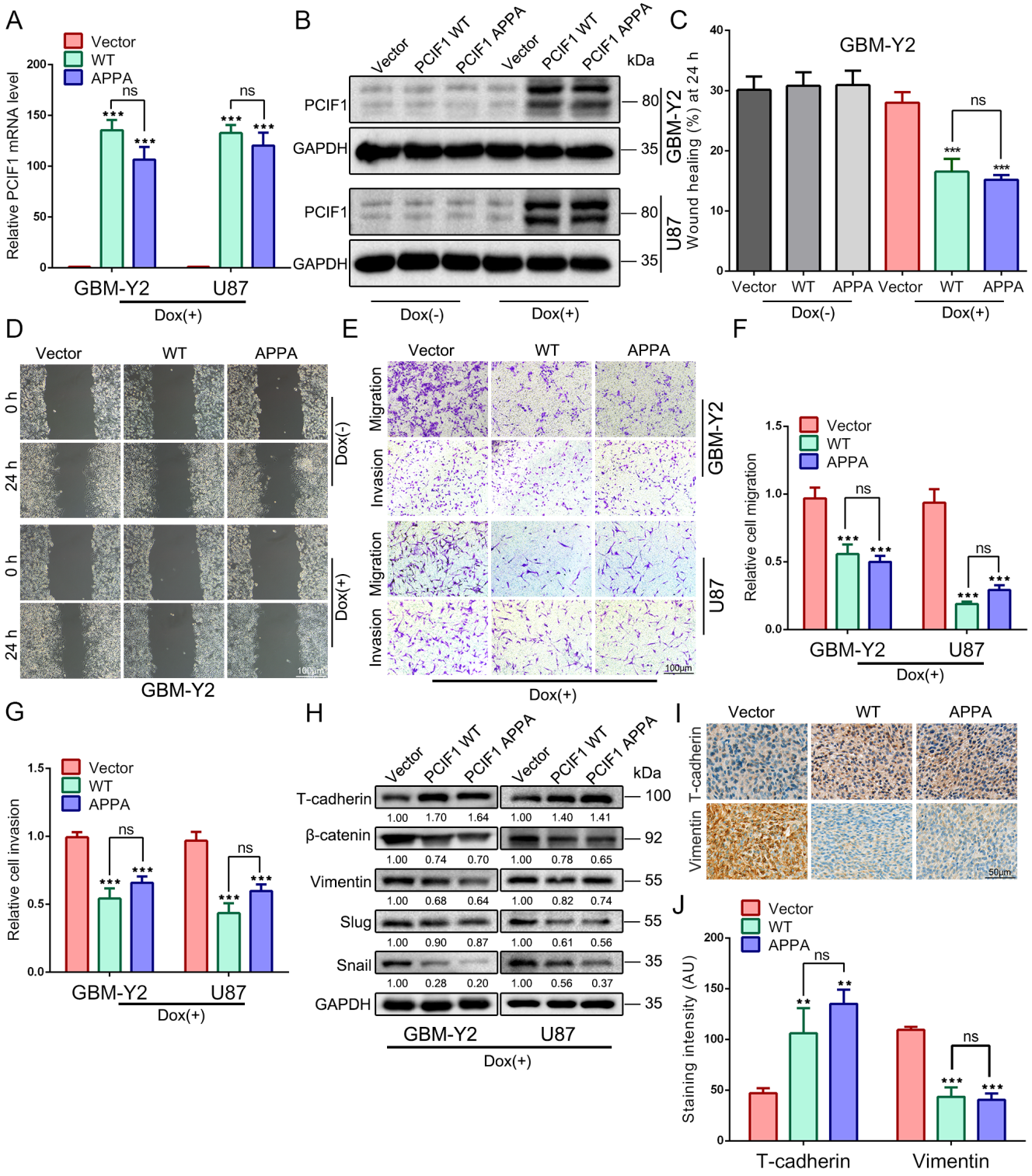


Figure 2. Analysis of PCIF1 overexpression in glioma cell migration, invasion, and EMT activation (A) qRT-PCR analysis of *PCIF1* mRNA expression in GBM-Y2 and U87 cells following PCIF1 overexpression. (B) WB analysis confirming PCIF1 protein expression in GBM-Y2 and U87 cells. (C,D) Scratch assay images of GBM-Y2 cells with PCIF1 overexpression at the 24 h time point, with quantification of wound healing percentage (C) and representative images (D). Scale bar = 100 μm. (E–G) Transwell migration and invasion assays assessing the migratory and invasive capacity of PCIF1-overexpressing GBM-Y2 and U87 cells, with representative images (E) and quantification of relative cell numbers (F,G). Scale bar = 100 μm. (H) WB analysis of EMT markers in GBM-Y2 and U87 cells following PCIF1 overexpression. (I,J) IHC staining of EMT markers in tumor samples from PCIF1-overexpressing glioma tissues, with representative images (I) and quantification of staining intensity (J). Scale bar = 50 μm for IHC images. Data are presented as the mean ± SEM of three independent experiments. Statistical significance compared to control groups is indicated by $*P < 0.05$, $**P < 0.01$, and $***P < 0.001$, and ns means no statistical significance.

dependent on its methyltransferase activity [19]. Together, these findings indicate that PCIF1 overexpression suppresses glioma cell migration and invasion, possibly by inhibiting EMT.

PCIF1 regulates AKT activation and phosphoinositide metabolism in glioma cells

To elucidate the effect of PCIF1 on AKT signaling in glioma cells, we first examined the changes in AKT and p-AKT expression upon PCIF1 modulation. WB analysis demonstrated that *PCIF1* knockdown led to increased total AKT levels and decreased p-AKT (Ser473) expression in U251 and T98G glioma cells (Figure 3A). In contrast, PCIF1 overexpression in U87 and GBM-Y2 cells resulted in decreased total AKT levels and enhanced p-AKT expression (Figure 3B). However, qRT-PCR analysis revealed no significant changes in AKT mRNA levels following PCIF1 depletion in U251 cells or overexpression in U87 cells, suggesting that PCIF1 may not regulate AKT by reducing protein synthesis (Figures 3C,D). We therefore explored the effect of PCIF1 on AKT stability using MG132 proteasomal inhibition and cycloheximide (CHX) chase assays. In U87 cells overexpressing PCIF1, MG132 treatment partially prevented AKT degradation, whereas CHX treatment failed to block AKT protein loss, suggesting that PCIF1 promotes AKT degradation via the proteasomal pathway (Figure 3E) [30]. In U251 cells with *PCIF1* knockdown, MG132 stabilized total AKT, whereas p-AKT levels remained decreased under both CHX and MG132 conditions (Figure 3F). To directly examine whether PCIF1 promotes AKT ubiquitination, we performed ubiquitination assays in U87 cells in the presence of MG132. Western blot analysis revealed a markedly increased HA-Ub signal in AKT immunoprecipitates from PCIF1-overexpressing cells compared with vector controls, indicating that PCIF1 enhances AKT ubiquitination (Figure 3G). These results indicate that PCIF1 regulates both the protein stability and phosphorylation level of AKT in glioma cells.

To further verify whether AKT activation mediates PCIF1-driven signaling, we treated *PCIF1*-knockdown U251 cells with the PI3K/AKT inhibitor LY294002 [31]. WB analysis showed that LY294002 treatment partially restored the EMT phenotype caused by *PCIF1* knockdown, i.e., increased T-cadherin expression and decreased expression of mesenchymal markers (β-catenin and Vimentin) (Figure 3H). PCIF1 contains a conserved WW domain, known for its ability to interact with proline-rich motifs in signaling molecules [11]. To assess whether this domain is involved in regulating AKT, we introduced both the APPA and S54H mutants and performed rescue experiments in PCIF1-depleted U251 cells [32,33]. WB analysis revealed that the WT and APPA constructs partially restored AKT and p-AKT levels, while the S54H mutant failed to do so, highlighting the importance of the WW domain in PCIF1-mediated AKT regulation (Figure 3I). A schematic diagram of PCIF1, illustrating its domain structure and the introduction of APPA (at the NPPF motif) and S54H (in the WW domain) mutations, is provided in Supplementary Figure S3.

Given the known interaction between AKT signaling and phosphoinositide metabolism, we assessed the effects of PCIF1 modulation on PI(3,4,5)P3 and PI(3,4)P2 levels. IF analysis showed that *PCIF1* knockdown in U251 cells significantly reduced PI(3,4,5)P3 levels. Conversely, PCIF1 overexpression in U87 cells resulted in increased PI(3,4,5)P3 levels (Figure 3J,K). Furthermore, ELISA revealed an increase in PI(3,4)P2 levels with *PCIF1* knockdown in U251 cells and decreased PI(3,4)P2 levels with PCIF1 overexpression in U87 cells (Figure 3L), further supporting the role of PCIF1 in regulating phosphoinositide metabolism [20,21].

Altogether, our results demonstrate that PCIF1 regulates AKT protein stability and activity and phosphoinositide metabolism, highlighting its essential function in glioma cell progression.

INPP5B downregulation mitigates the effects of *PCIF1* knockdown on glioma cell migration, invasion, and AKT signaling

INPP5B dephosphorylates PI(3,4,5)P3 to PI(3,4)P2, which are critical mediators of AKT signaling. We therefore examined the functional relationship between PCIF1 and INPP5B [20]. First, we assessed INPP5B expression in PCIF1-depleted glioma cells. qRT-PCR and WB analyses revealed that *PCIF1* knockdown significantly increased *INPP5B* mRNA (Figure 4A) and protein (Figure 4B) levels in U251 and T98G cells. IHC staining further confirmed these findings, showing elevated INPP5B expression in xenograft glioma tissues from the PCIF1-depleted models (Figure 4C) [19]. These data indicate that PCIF1 negatively regulates INPP5B expression in gliomas. Second, we evaluated the effect of *INPP5B* knockdown on phosphoinositide metabolism changes caused by PCIF1 depletion. IF analysis revealed that si-*INPP5B4* increased PI(3,4,5)P3 levels in PCIF1-depleted U251 cells (Figure 4D,E), while ELISAs confirmed a significant reduction in PI(3,4)P2 levels (Figure 4F) [20,21]. Furthermore, WB analysis demonstrated that *INPP5B* knockdown in PCIF1-depleted U251 cells resulted in an increase in both total AKT and p-AKT (Ser473) levels (Figure 4G), suggesting that INPP5B depletion promotes AKT activation through the accumulation of PI(3,4,5)P3. Importantly, *INPP5B* knockdown did not affect PCIF1 expression, confirming that INPP5B acts downstream of PCIF1 in this signaling pathway. Third, we investigated whether INPP5B mediates the migratory and invasive properties induced by PCIF1 depletion. Functional rescue experiments were performed using si-*INPP5B4* in *PCIF1*-knockdown U251 cells. Scratch assays at the 24 h time point demonstrated that si-*INPP5B4* significantly attenuated the wound-healing ability of these cells, indicating that INPP5B is essential for the enhanced migration observed following *PCIF1* knockdown (Figure 4H,I). In parallel, Transwell assays revealed that INPP5B downregulation significantly reduced both migration and invasion (Figure 4J,K) in *PCIF1*-depleted U251 cells. Finally, we assessed the role of INPP5B in modulating EMT phenotype. WB analysis showed that INPP5B depletion significantly decreased mesenchymal markers (β-catenin and Vimentin) while increasing the expression of the epithelial marker T-cadherin (Figure 4L). Notably, when both PCIF1 and INPP5B were simultaneously depleted, we observed a modest increase in T-cadherin level and a decrease in β-catenin level compared with control + si-*INPP5B4*. This may reflect a context-dependent compensatory response to dual loss, which partially restores epithelial marker expression while dampening mesenchymal signaling. These results indicate that INPP5B is involved in the EMT process associated with *PCIF1* knockdown and suggest that INPP5B downregulation can reverse the aggressive migratory and invasive properties induced by PCIF1 depletion.

Altogether, these findings provide evidence that INPP5B is a key downstream effector of PCIF1, mediating its effects on phosphoinositide metabolism, AKT signaling, and glioma cell migration and invasion.

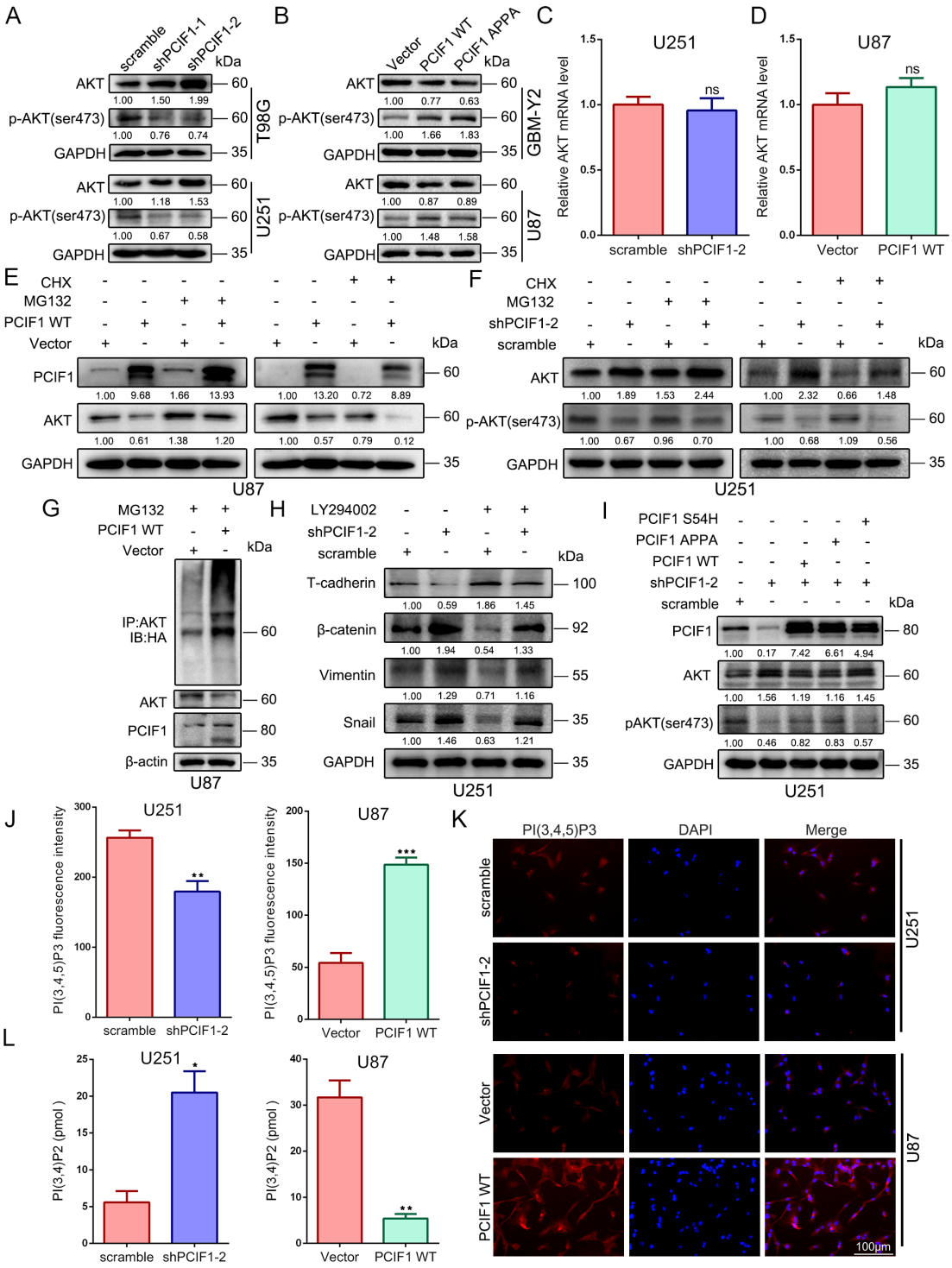


Figure 3. PCIF1 regulation of AKT signaling and phosphoinositide metabolism in glioma cells (A,B) WB analysis of total AKT and p-AKT (Ser473) expression in U251 and T98G *PCIF1* knockdown cells (A) and in U87 and GBM-Y2 PCIF1 overexpression cells (B). (C,D) qRT-PCR analysis of *AKT* mRNA levels in *PCIF1*-knockdown U251 cells (C) and PCIF1-overexpressing U87 cells (D). (E,F) WB analysis of total AKT and p-AKT (Ser473) levels following MG132 and CHX treatment in PCIF1-overexpressing U87 cells (E) and (F) U251 cells with *PCIF1* knockdown. (G) WB analysis of AKT ubiquitination in PCIF1-overexpressing U87 cells treated with MG132. (H) WB analysis of EMT markers in *PCIF1*-knockdown U251 cells treated with LY294002. (I) WB analysis of total AKT and p-AKT (Ser473) levels in *PCIF1*-knockdown U251 cells transfected with WT PCIF1, APPA, or S54H mutants. (J,K) IF staining of PI(3,4,5)P3 in *PCIF1*-knockdown U251 cells and PCIF1-overexpressing U87 cells, with quantification of fluorescence intensity (J) and representative images (K). Scale bars = 100 μm. (L) ELISA showing PI(3,4)P2 levels (pmol) in *PCIF1*-knockdown U251 cells and PCIF1-overexpressing U87 cells. Data are presented as the mean ± SEM of three independent experiments for all assays, with the ELISA performed in two independent experiments. Statistical significance compared to control groups is indicated by $^{*}P < 0.05$, $^{**}P < 0.01$, and $^{***}P < 0.001$, and ns means no statistical significance.

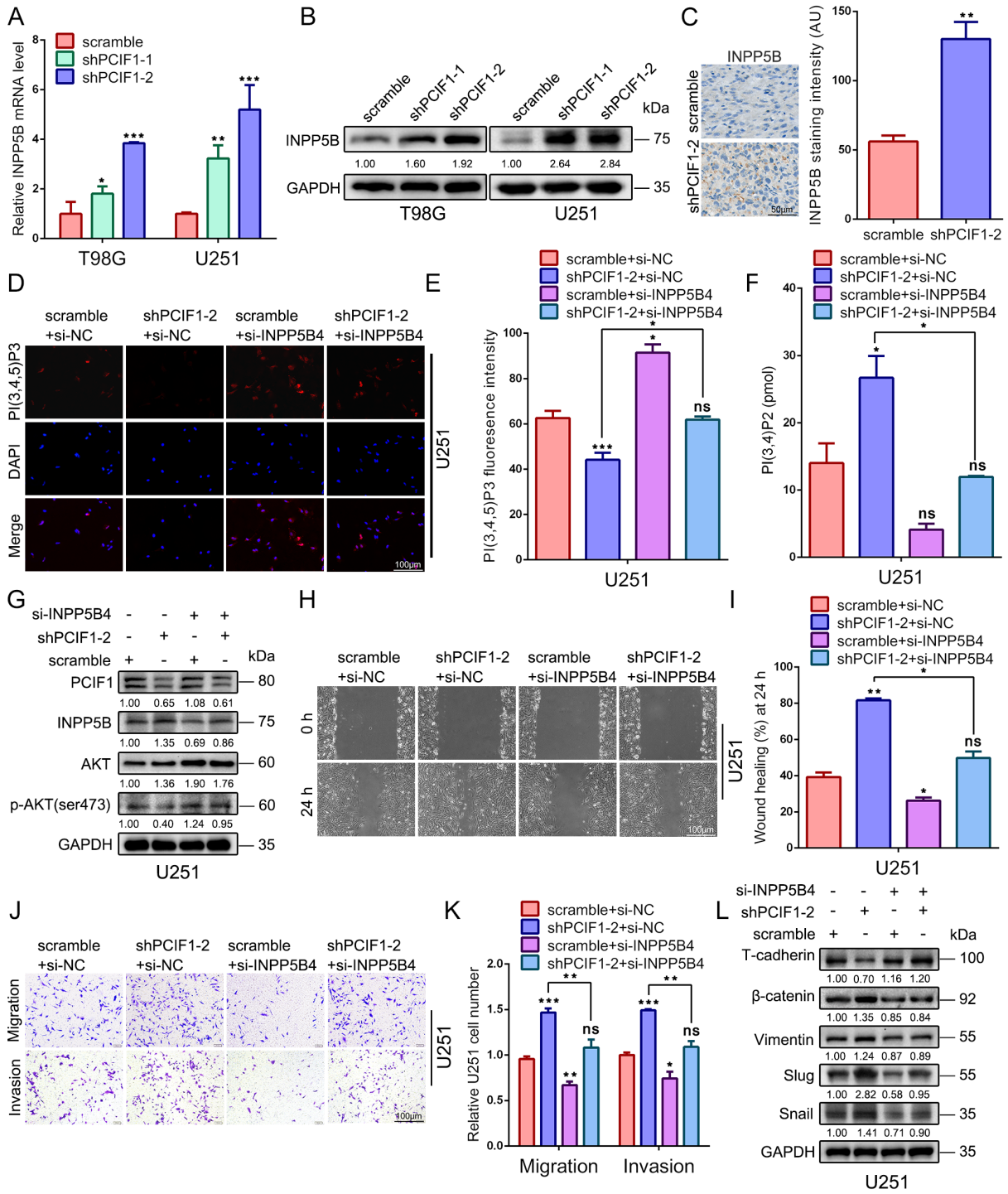


Figure 4. INPP5B modulation restores glioma cell migration, invasion, and AKT signaling in PCIF1-depleted cells (A) qRT-PCR analysis of *INPP5B* mRNA expression in U251 and T98G cells with *PCIF1* knockdown. (B) WB analysis of INPP5B protein levels in T98G and U251 cells after *PCIF1* knockdown. (C) IHC staining of INPP5B in glioma tissues from PCIF1-depleted models. Scale bar = 50 μm. (D, E) IF staining of PI(3,4,5)P3 in U251 cells with PCIF1 knockdown and INPP5B downregulation, with representative images (D) and quantification of fluorescence intensity (E). Scale bars = 100 μm. (F) ELISA analysis of PI(3,4)P2 levels (pmol) in U251 cells with *PCIF1* knockdown and INPP5B downregulation. (G) WB analysis of total AKT and p-AKT (Ser473) in U251 cells with *PCIF1* knockdown and INPP5B downregulation. (H, I) Scratch assay of U251 cells with *PCIF1* knockdown at the 24 h time point, with representative images (H) and quantification of wound healing percentage (I). Scale bar = 100 μm. (J,K) Transwell migration and invasion assays of U251 cells with *PCIF1* knockdown and INPP5B downregulation, with representative images (J) and quantification of relative cell number (K). Scale bar = 100 μm. (L) WB analysis of EMT markers in U251 cells with *PCIF1* knockdown and INPP5B downregulation. Data are presented as the mean ± SEM of three independent experiments for all assays, with the ELISA performed in two independent experiments. Statistical significance compared to control groups is indicated by $*P < 0.05$, $**P < 0.01$, and $***P < 0.001$, and ns means no statistical significance.

INPP5B overexpression reverses the effects of PCIF1 on glioma cell aggressiveness and AKT signaling

We first assessed the impact of PCIF1 overexpression on INPP5B expression in glioma cells. qRT-PCR and WB analyses revealed that PCIF1 overexpression significantly reduced both *INPP5B* mRNA (Figure 5A) and protein (Figure 5B) levels in U87 and GBM-Y2 cells. Next, we investigated whether INPP5B overexpression could rescue the changes in phosphoinositide metabolism and AKT signaling caused by PCIF1 overexpression. IF assays showed that INPP5B overexpression significantly decreased PI(3,4,5)P3 fluorescence intensity (Figure 5C,D). In contrast, ELISAs confirmed that PCIF1-overexpressing U87 cells with INPP5B overexpression exhibited increased PI(3,4)P2 levels (Figure 5E). To assess the effects of INPP5B overexpression on AKT signaling, we performed western blot analysis and found that INPP5B overexpression in PCIF1-overexpressing U87 cells led to a reduction in both total AKT and p-AKT (Ser473) levels (Figure 5F), supporting the idea that INPP5B modulates PI(3,4,5)P3 availability, thereby influencing downstream AKT signaling. Notably, INPP5B overexpression did not affect PCIF1 expression, reinforcing that PCIF1 acts upstream of INPP5B in this pathway. Next, we explored whether INPP5B overexpression could rescue the migratory and invasive properties of glioma cells overexpressing PCIF1. Scratch assays revealed that INPP5B overexpression significantly enhanced the wound-healing ability of GBM-Y2 cells with PCIF1 upregulation at the 24 h time point post-scratch (Figure 5G,H). Similarly, Transwell migration and invasion assays demonstrated that INPP5B overexpression significantly enhanced migration and invasion (Figure 5I,J) in U87 cells overexpressing PCIF1. Finally, we assessed the role of INPP5B in regulating the EMT phenotype. Western blot analysis demonstrated that INPP5B overexpression increased mesenchymal markers (β-catenin and Vimentin) while decreasing the expression of the epithelial marker T-cadherin in U87 cells overexpressing PCIF1 (Figure 5K).

In summary, these findings suggest that PCIF1 overexpression suppresses INPP5B expression, leading to significant alterations in phosphoinositide metabolism, AKT pathway activation, and a corresponding reduction in glioma cell migration and invasion.

Discussion

This study uncovers the multifaceted role of PCIF1 in glioma progression, demonstrating its impact on cell migration, invasion, EMT, and the AKT signaling pathway. Our findings establish PCIF1 as a key suppressor of glioma cell motility, where its down-regulation enhances migration and invasion, whereas its over-expression inhibits these processes. Consistently, we previously reported that PCIF1 overexpression reduced proliferation, induced G2/M phase cell cycle arrest, and promoted apoptosis in glioma cells [19]. In addition, analysis of glioma datasets (GSE16011, CGGA-325, and CGGA-693) and our patient cohort showed that PCIF1 expression decreased with increasing tumor grade [19], supporting its role in restraining glioma aggressiveness. Taken together, these findings suggest that PCIF1 is a potent regulator of cellular mechanisms vital for glioma progression, positioning it as a promising target for glioma treatment.

Structurally, PCIF1 harbors a conserved NPPF motif essential for its m^6Am methyltransferase activity, which influences mRNA stability and translation [9,10]. Although loss of PCIF1 in melanoma cells disrupts m^6Am levels, our findings reveal that PCIF1 suppresses glioma migration and invasion through a mechanism independent of its methyltransferase function. Overexpression of the catalytically inactive PCIF1 (APPA mutant) had no significant effect on glioma migration and invasion compared to wild-type PCIF1. Given that methyltransferase activity is not the key determinant here, other domains of PCIF1 may contribute to its effects on glioma cell mobility. One potential candidate is the WW domain, which interacts with the phosphorylated C-terminal domain (CTD) of RNA polymerase II, allowing it to associate with transcriptional regulation [11]. Our recent publication demonstrated that the WW domain plays a crucial role in PCIF1-mediated inhibition of glioma growth [26]. Further investigations into the WW domain could provide valuable insights into its contribution to the mobility and invasive behavior of glioma cells.

EMT is crucial for enhancing glioma cell motility and invasiveness by promoting a mesenchymal phenotype [34]. Loss of PCIF1 is associated with the upregulation of mesenchymal markers (Vimentin, β-catenin, Snail, and Slug) and the downregulation of epithelial markers (T-cadherin), indicating its role in EMT [34]. These findings highlight a direct link between PCIF1 expression and glioma aggressiveness through EMT modulation. Additionally, structural changes in PCIF1-depleted cells were evident in cytoskeletal reorganization. TRITC-phalloidin staining revealed an increase in actin stress fibers and filopodium formation, suggesting enhanced cytoskeletal remodeling. These structural changes are hallmarks of enhanced cell motility, facilitating cellular migration and invasion [28]. The observed reorganization of the actin network reflects a more dynamic and invasive phenotype in PCIF1-depleted cells, supporting the hypothesis that PCIF1 loss promotes glioma aggressiveness by enhancing cytoskeletal remodeling.

Mechanistically, PCIF1 overexpression leads to a decrease in total AKT levels while increasing p-AKT levels, suggesting a complex regulation of AKT activity. However, rather than driving glioma aggressiveness, this paradoxical effect on AKT protein levels and activity by PCIF1 may contribute to a regulatory balance that suppresses glioma cell motility. Importantly, our results suggest that PCIF1-mediated upregulation of p-AKT is probably part of a feedback loop caused by reduced total AKT level, which modulates the AKT pathway. CHX and MG132 treatments further suggested that PCIF1-mediated regulation of AKT involves proteasome-dependent degradation [30]. CHX treatment in PCIF1-overexpressing cells resulted in a shortened AKT half-life, while MG132 treatment partially restored AKT level, confirming that proteasomal degradation contributes to AKT regulation. Similarly, in *PCIF1*-knockdown cells, MG132 stabilized total AKT, but p-AKT levels remained decreased under both CHX and MG132 treatments, indicating that reduced PCIF1 also impairs AKT stability via the proteasomal pathway. Consistently, ubiquitination assays performed in the presence of MG132 showed that PCIF1 enhances AKT ubiquitination, providing mechanistic evidence that PCIF1 directly fine-tunes AKT signaling via proteasomal regulation. Furthermore, pharmacological inhibition of the PI3K/AKT pathway with LY294002 in PCIF1-depleted cells provided functional evidence that AKT acts as a critical downstream mediator of PCIF1 signaling [31]. Inhibition of AKT activity partially reversed the mesenchymal phenotype induced by *PCIF1* knockdown. These findings underscore the dependence of PCIF1-driven EMT on AKT signaling and further support the notion that PCIF1 modulates glioma behavior primarily through the AKT pathway. By promoting

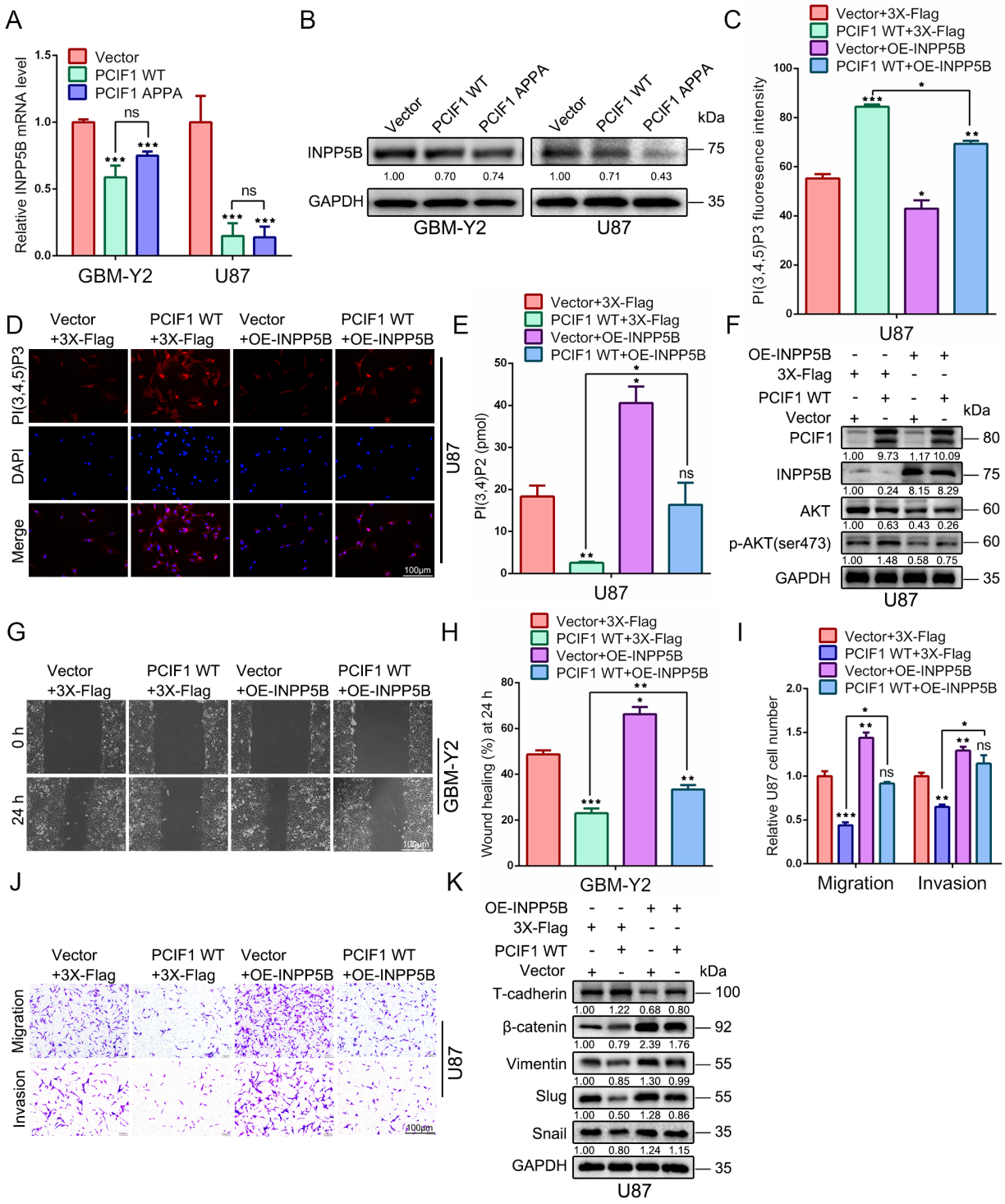


Figure 5. INPP5B overexpression reverses the effects of PCIF1 upregulation in glioma cells (A) qRT-PCR analysis of *INPP5B* mRNA expression in U87 and GBM-Y2 cells overexpressing PCIF1. (B) WB analysis confirming INPP5B protein expression in GBM-Y2 and U87 cells. (C, D) IF staining of PI(3,4,5)P3 in U87 cells with PCIF1 overexpression and INPP5B overexpression, with quantification of fluorescence intensity (C) and representative images (D). Scale bar = 100 μm. (E) ELISA analysis of PI(3,4)P2 levels (pmol) in U87 cells with PCIF1 overexpression and INPP5B overexpression. (F) WB analysis of total AKT and p-AKT (Ser473) in U87 cells with PCIF1 overexpression and INPP5B overexpression. (G,H) Scratch assay of GBM-Y2 cells with PCIF1 overexpression at the 24 h time point, with representative images (G) and quantification of wound healing percentage (H). Scale bar = 100 μm. (I,J) Transwell migration and invasion assays of U87 cells with PCIF1 overexpression and INPP5B overexpression, with quantification of relative cell number (I) and representative images (J). Scale bar = 100 μm. (K) WB analysis of EMT markers in U87 cells with PCIF1 overexpression and INPP5B overexpression. Data are presented as the mean ± SEM of three independent experiments for all assays, with the ELISA performed in two independent experiments. Statistical significance compared to control groups is indicated by $*P < 0.05$, $**P < 0.01$, and $***P < 0.001$, and ns means no statistical significance.

AKT activation while suppressing glioma cell migration and invasion, PCIF1 may help maintain a balance that inhibits tumor cell motility and invasiveness without completely suppressing AKT activity, which is crucial for maintaining cellular functions. These observations highlight the intricate role of PCIF1 in modulating AKT signaling during glioma progression.

In gliomas, mutations, deletions, or epigenetic silencing of tumor suppressor genes contribute to the hyperactivation of AKT signaling pathways [35]. Given the critical role of PI(3,4,5)P3 and PI(3,4)P2 as second messengers in AKT signaling, we found that PCIF1 overexpression enhances PI(3,4,5)P3 levels while reducing PI(3,4)P2 level, whereas *PCIF1* knockdown produces the opposite effect [21]. This shift from PI(3,4,5)P3 to PI(3,4)P2 correlates with changes in p-AKT levels, as PI(3,4,5)P3 serves as a primary second messenger that activates AKT [21]. These findings suggest that PCIF1 serves as a negative regulator of PI(3,4)P2 accumulation, possibly compensating for the loss of tumor suppressive regulation in glioblastoma. Furthermore, PCIF1 contains an N-terminal WW domain, which interacts with the phosphorylated CTD of RNA polymerase II, allowing it to associate with transcription start sites [11]. The S54H mutation within the WW domain disrupts its ability to bind to the phosphorylated CTD, impairing its regulatory function [32,33]. Rescue experiments in *PCIF1*-knockdown glioma cells demonstrated that wild-type PCIF1 and the APPA mutant could partially restore AKT and p-AKT levels, whereas the S54H mutant failed, underscoring the importance of the WW domain in glioma cell migration and invasion.

INPP5B, an inositol 5-phosphatase, hydrolyzes PI(3,4,5)P3 to PI(3,4)P2, modulating AKT signaling [20]. In line with the effect of PCIF1 on the PI(3,4,5)P3 to PI(3,4)P2 transition, we observed that PCIF1 downregulation elevates INPP5B expression, whereas PCIF1 overexpression reduces INPP5B level, leading to an accumulation of PI(3,4,5)P3 and a decrease in PI(3,4)P2. These findings suggest that PCIF1 may regulate phosphoinositide metabolism by affecting PI phosphatase INPP5B expression. Interestingly, INPP5B inhibition in *PCIF1*-knockdown cells restored PI(3,4,5)P3, reduced PI(3,4)P2, and increased p-AKT. Conversely, INPP5B overexpression reversed the effects of PCIF1 overexpression, reducing PI(3,4,5)P3, increasing PI(3,4)P2, and further suppressing p-AKT, thereby enhancing glioma cell aggressiveness. Therefore, the compensatory increase in p-AKT caused by PCIF1 overexpression may be attributed to changes in both INPP5B expression and phosphoinositide metabolism.

In summary, given the complexity of glioma biology, therapeutic strategies targeting PCIF1 or its downstream effectors may face challenges due to the activation of compensatory signaling pathways, potentially limiting the effectiveness of monotherapies. This highlights the importance of considering combination therapies that target multiple pathways to overcome resistance and improve therapeutic outcomes. As illustrated in Figure 6, PCIF1's regulation of AKT signaling and EMT is central to its role in glioma progression, which further emphasizes the need to explore combination therapies. Taken together, our mechanistic data and previous clinical analyses suggest that PCIF1 may serve as a modulator of glioma aggressiveness in patients, linking its molecular effects to tumor malignancy and metastatic behavior, even if its impact on overall survival requires further study [19]. Future studies exploring the synergistic effects of PCIF1 modulation with existing treatments, such as AKT inhibitors or other signaling pathway inhibitors, may offer novel approaches to preventing glioma progression more effectively.

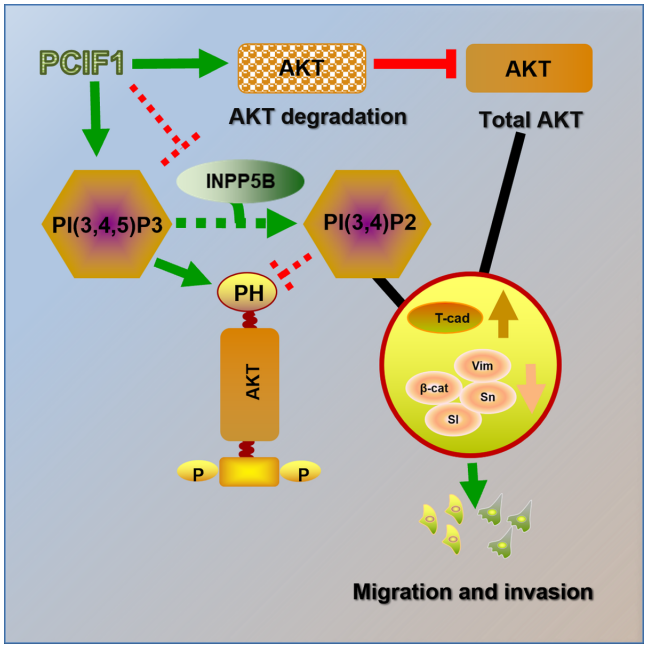


Figure 6. Schematic representation of PCIF1-mediated regulation of glioma cell migration, invasion, and EMT via AKT signaling and phosphoinositide dynamics This schematic illustrates how PCIF1 modulates glioma cell motility, invasion, and epithelial-to-mesenchymal transition (EMT) through its regulation of AKT signaling and phosphoinositide metabolism. PCIF1 promotes AKT degradation via the proteasomal pathway, thereby reducing total AKT levels and suppressing EMT, while the increase in phosphorylated AKT (p-AKT) may reflect a compensatory response. PCIF1 influences the balance between PI(3,4,5)P3 and PI(3,4)P2 by modulating INPP5B, an inositol 5-phosphatase that converts PI(3,4,5)P3 to PI(3,4)P2 and is downregulated by PCIF1. This phosphoinositide equilibrium regulates AKT activation, as PI(3,4,5)P3 binds to the pleckstrin homology (PH) domain of AKT, promoting its phosphorylation at Ser473 (p-AKT), which is essential for its activation. Additionally, PCIF1 regulates EMT, where its overexpression suppresses mesenchymal markers while promoting epithelial markers, reducing glioma cell invasiveness. Conversely, PCIF1 depletion induces a mesenchymal shift, enhancing cell motility and invasion. The schematic highlights INPP5B as a key downstream mediator of PCIF1, linking phosphoinositide signaling to AKT activation and EMT regulation. Activation pathways are depicted with green arrows, inhibitory effects with red arrows, and regulatory interactions with dotted lines. The yellow "P" on AKT denotes phosphorylation at Ser473. This model underscores the central role of PCIF1 in modulating AKT signaling and EMT, integrating AKT degradation, phosphoinositide dynamics, and EMT suppression to control glioma progression.

Our study reveals that PCIF1 plays a pivotal role in inhibiting glioma progression by modulating migration, invasion, and AKT signaling pathways. Specifically, PCIF1 regulates INPP5B expression, which influences glioma aggressiveness by modulating AKT stability, activity, and phosphoinositide metabolism. Notably, both wild-type PCIF1 and the APPA mutant showed similar effects on migration and invasion, indicating that this inhibitory function on glioma cell motility and invasiveness is not entirely dependent on its methyltransferase activity. These findings position PCIF1 as a promising therapeutic target, and further research into its role along with its interaction with INPP5B in glioma biology is warranted for the development of novel treatment strategies.

Supplementary Data

Supplementary data are available at *Acta Biochimica et Biophysica Sinica* online.

Data Availability

The data supporting the findings of this study are available from the corresponding authors upon reasonable requests.

Funding

This work was supported by the grants from the National Natural Science Foundation of China (Nos. 82072763, 82473218, and 82501654), the Construction Project of High-Level Hospital of Jiangsu Province (No. 2023601001), the Key Research & Development Plan of Xuzhou City (No. KC22103), the Advanced Program of the Affiliated Hospital of Xuzhou Medical University (No. PYJH2024206), and the Clinical Research Special Project of the Affiliated Hospital of Xuzhou Medical University (No. LCZX202409).

Conflict of Interest

The authors declare that they have no conflict of interest.

References

1. Tan AC, Ashley DM, López GY, Malinzak M, Friedman HS, Khasraw M. Management of glioblastoma: state of the art and future directions. *CA Cancer J Clin* 2020, 70: 299–312
2. Pandey N, Anastasiadis P, Carney CP, Kanvinde PP, Woodworth GF, Winkles JA, Kim AJ. Nanotherapeutic treatment of the invasive glioblastoma tumor microenvironment. *Adv Drug Deliv Rev* 2022, 188: 114415
3. Wu W, Klockow JL, Zhang M, Lafortune F, Chang E, Jin L, Wu Y, *et al.* Glioblastoma multiforme (GBM): an overview of current therapies and mechanisms of resistance. *Pharmacol Res* 2021, 171: 105780
4. Dakal TC, Kakde GS, Maurya PK. Genomic, epigenomic and transcriptomic landscape of glioblastoma. *Metab Brain Dis* 2024, 39: 1591–1611
5. Khabibov M, Garifullin A, Boumber Y, Khaddour K, Fernandez M, Khamitov F, Khalikova L, *et al.* Signaling pathways and therapeutic approaches in glioblastoma multiforme (review). *Int J Oncol* 2022, 60: 69
6. Cai Q, Zhou W, Wang W, Dong B, Han D, Shen T, Creighton CJ, *et al.* MAPK6-AKT signaling promotes tumor growth and resistance to mTOR kinase blockade. *Sci Adv* 2021, 7: eabi6439
7. Fontana F, Giannitti G, Marchesi S, Limonta P. The PI3K/Akt pathway and glucose metabolism: a dangerous liaison in cancer. *Int J Biol Sci* 2024, 20: 3113–3125
8. White J, White MPJ, Wickremesekera A, Peng L, Gray C. The tumour microenvironment, treatment resistance and recurrence in glioblastoma. *J Transl Med* 2024, 22: 540
9. Boulias K, Toczydłowska-Socha D, Hawley BR, Liberman N, Takashima K, Zaccara S, Guez T, *et al.* Identification of the m^{6}Am methyltransferase PCIF1 reveals the location and functions of m^{6}Am in the transcriptome. *Mol Cell* 2019, 75: 631–643.e8
10. Yu D, Zhou J, Chen Q, Wu T, Blumenthal RM, Zhang X, Cheng X. Enzymatic characterization of *in vitro* activity of RNA methyltransferase PCIF1 on DNA. *Biochemistry* 2022, 61: 1005–1013
11. Fan H, Sakuraba K, Komuro A, Kato S, Harada F, Hirose Y. PCIF1, a novel human WW domain-containing protein, interacts with the phosphorylated RNA polymerase II. *Biochem Biophys Res Commun* 2003, 301: 378–385
12. Li K, Chen J, Zhang C, Cheng M, Chen S, Song W, Yang C, *et al.* The CTBP2-PCIF1 complex regulates m6Am modification of mRNA in head and neck squamous cell carcinoma. *J Clin Invest* 2023, 133: e170173
13. Zhuo W, Sun M, Wang K, Zhang L, Li K, Yi D, Li M, *et al.* m6Am methyltransferase PCIF1 is essential for aggressiveness of gastric cancer cells by inhibiting TM9SF1 mRNA translation. *Cell Discov* 2022, 8: 48
14. Luo W, Xu Z, Li F, Ding L, Wang R, Lin Y, Mao X, *et al.* m6Am methyltransferase PCIF1 promotes LPP3 mediated phosphatidic acid metabolism and renal cell carcinoma progression. *Adv Sci* 2024, 11: e2404033
15. Wang L, Wu L, Zhu Z, Zhang Q, Li W, Gonzalez GM, Wang Y, *et al.* Role of PCIF1-mediated 5′-cap N6-methyladeonsine mRNA methylation in colorectal cancer and anti-PD-1 immunotherapy. *EMBO J* 2023, 42: e111673
16. Hensel J, Duex JE, Owens C, Dancik GM, Edwards MG, Frierson HF, Theodorescu D. Patient mutation directed shRNA screen uncovers novel bladder tumor growth suppressors. *Mol Cancer Res* 2015, 13: 1306–1315
17. An H, Hong Y, Goh YT, Koh CWQ, Kanwal S, Zhang Y, Lu Z, *et al.* m6Am sequesters PCF11 to suppress premature termination and drive neuroblastoma differentiation. *Mol Cell* 2024, 84: 4142–4157.e14
18. Sendinc E, Valle-Garcia D, Dhall A, Chen H, Henriques T, Navarrete-Perea J, Sheng W, *et al.* PCIF1 catalyzes m6Am mRNA methylation to regulate gene expression. *Mol Cell* 2019, 75: 620–630.e9
19. Gao S, Zhou J, Hu Z, Zhang S, Wu Y, Musunuru PP, Zhang T, *et al.* Effects of the m6Am methyltransferase PCIF1 on cell proliferation and survival in gliomas. *Biochim Biophys Acta Mol Basis Dis* 2022, 1868: 166498
20. Davis WJ, Lehmann PZ, Li W. Nuclear PI3K signaling in cell growth and tumorigenesis. *Front Cell Dev Biol* 2015, 3: 24
21. Ma K, Cheung SM, Marshall AJ, Duronio V. PI(3,4,5)P3 and PI(3,4)P2 levels correlate with PKB/Akt phosphorylation at Thr308 and Ser473, respectively; PI(3,4)P2 levels determine PKB activity. *Cell Signal* 2008, 20: 684–694
22. Wang X, Wang Z, Zhang Y, Wang Y, Zhang H, Xie S, Xie P, *et al.* Golgi phosphoprotein 3 sensitizes the tumour suppression effect of gefitinib on gliomas. *Cell Prolif* 2019, 52: e12636
23. You F, Li C, Zhang S, Zhang Q, Hu Z, Wang Y, Zhang T, *et al.* Sitagliptin inhibits the survival, stemness and autophagy of glioma cells, and enhances temozolomide cytotoxicity. *Biomed Pharmacother* 2023, 162: 114555
24. Zhang T, Ji D, Wang P, Liang D, Jin L, Shi H, Liu X, *et al.* The atypical protein kinase RIOK3 contributes to glioma cell proliferation/survival, migration/invasion and the AKT/mTOR signaling pathway. *Cancer Lett* 2018, 415: 151–163
25. Sha Z, Zhou J, Wu Y, Zhang T, Li C, Meng Q, Musunuru PP, *et al.* BYSL promotes glioblastoma cell migration, invasion, and mesenchymal transition through the GSK-3β/β-catenin signaling pathway. *Front Oncol* 2020, 10: 565225
26. Yin J, Liu G, Zhou Y, Zhou J, Guo M, Hu Z, Musunuru PP, *et al.* The WW domain presents a promising target for the development of PCIF1 agonists in the treatment of glioma. *npj Precis Onc* 2025, 9: 329
27. Gao S, Sha Z, Zhou J, Wu Y, Song Y, Li C, Liu X, *et al.* BYSL contributes to tumor growth by cooperating with the mTORC2 complex in gliomas. *Cancer Biol Med* 2021, 18: 88–104
28. Mannherz HG, Budde H, Jarkas M, Hassoun R, Malek-Chudzik N, Mazur AJ, Skuljec J, *et al.* Reorganization of the actin cytoskeleton during the formation of neutrophil extracellular traps (NETs). *Eur J Cell Biol* 2024, 103: 151407
29. Noronha C, Ribeiro AS, Taipa R, Castro DS, Reis J, Faria C, Paredes J. Cadherin expression and EMT: a focus on gliomas. *Biomedicines* 2021, 9:

1328
30. Adachi M, Katsumura KR, Fujii K, Kobayashi S, Aoki H, Matsuzaki M. Proteasome-dependent decrease in Akt by growth factors in vascular smooth muscle cells. *FEBS Lett* 2003, 554: 77–80
31. Lv Y, Huang Q, Dai W, Jie Y, Yu G, Fan X, Wu A, *et al.* AQP9 promotes astrocytoma cell invasion and motility via the AKT pathway. *Oncol Lett* 2018, 16: 6059–6064
32. Hirose Y, Iwamoto Y, Sakuraba K, Yunokuchi I, Harada F, Ohkuma Y. Human phosphorylated CTD-interacting protein, PCIF1, negatively modulates gene expression by RNA polymerase II. *Biochem Biophys Res Commun* 2008, 369: 449–455
33. Zhang Q, Kang Y, Wang S, Gonzalez GM, Li W, Hui H, Wang Y, *et al.* HIV reprograms host m6Am RNA methylome by viral Vpr protein-mediated degradation of PCIF1. *Nat Commun* 2021, 12: 5543
34. Iwadate Y. Epithelial-mesenchymal transition in glioblastoma progression. *Oncol Lett* 2016, 11: 1615–1620
35. Prakash V, Gabrani R. Epigenetic dysregulation in glioblastoma: potential pathways to precision medicine. *Neurogenetics* 2024, 26: 5